Supporting Information

Two-Photon based Pulse Autocorrelation with CdSe Nanoplatelets

Michael T. Quick,[†] Nina Owschimikow,[†] Ali Hossain Khan,[‡,¶] Anatolii

Polovitsyn,[‡,¶] Iwan Moreels,[‡,¶] Ulrike Woggon,[†] and Alexander W. Achtstein[*,†]

[†]*Institute of Optics and Atomic Physics, Technical University of Berlin, Strasse des 17. Juni 135,*

10623 Berlin, Germany

[‡]*Instituto Italiano di Tecnologia, via morego 30, 16163 Genova, Italy*

[¶]*Department of Chemistry, Ghent University, krijgslaan 281-S3, 9000 Gent, Belgium*

E-mail: achtstein@tu-berlin.de

Fax: +49(0)30 31421079

Linear Absorbance and Volume Fraction

CdSe nanoplatelets (NPLs) of 4.5 monolayers thickness (a single monolayer is $\sim$0.305 nm) and 24x12 nm^2 and 29x6 nm^2 lateral size were dispersed in a polystyrene matrix. Their synthesis is described in Ref. 1. Size and shape of the NPLs were determined by TEM-images, see figs. 1 and 2, respectively. We remark that TEM was done with the platelet dispersion, dried on TEM grids. Stacking does not occur in the polystyrene embedded samples.

Figure 3 shows the linear absorption of the used CdSe nanoplatelets (NPLs). Follow-ing Hens et al.[2] the volume fraction can be estimated by
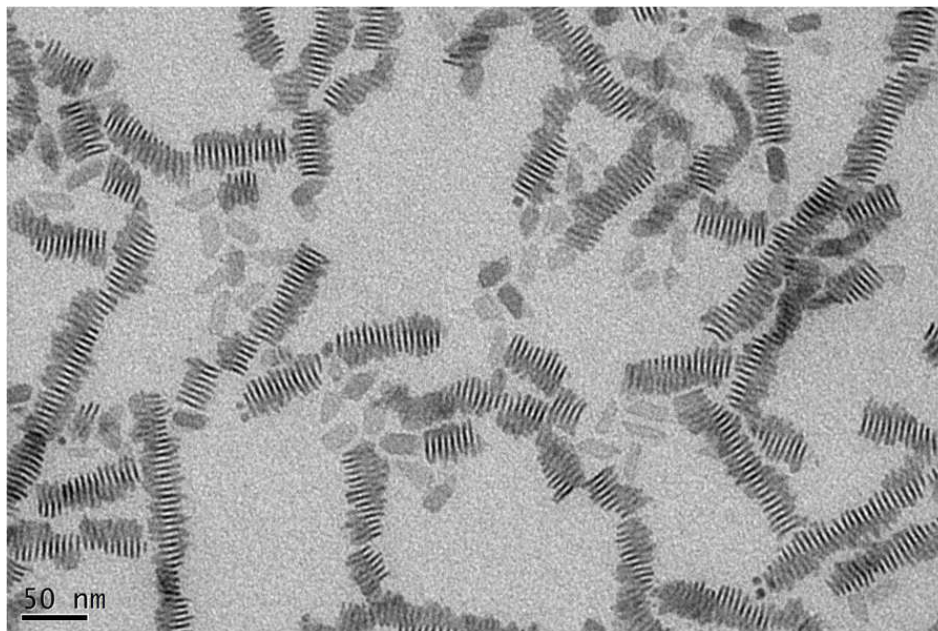
Figure 1: TEM of 24x12 nm^2 NPLs.
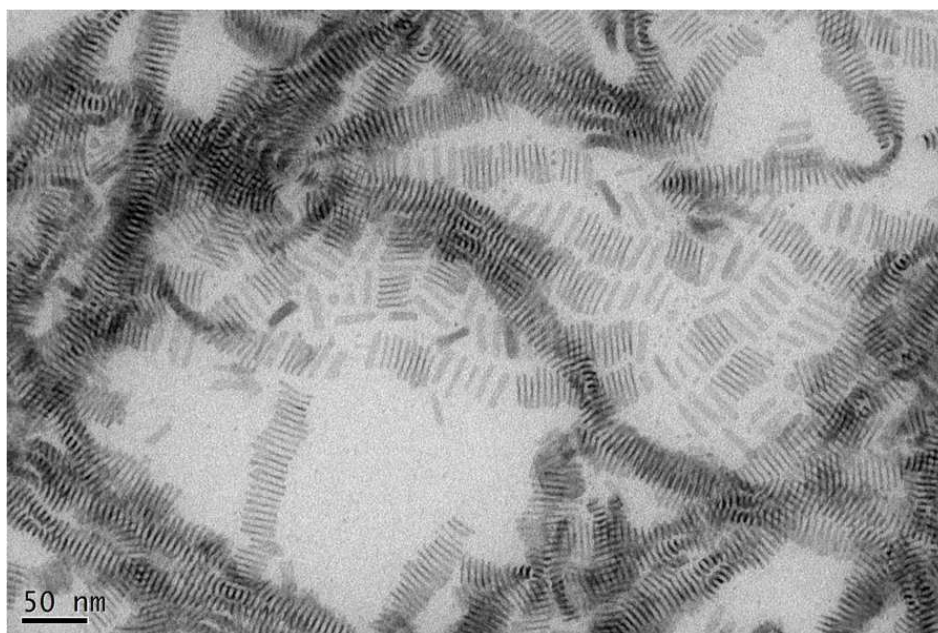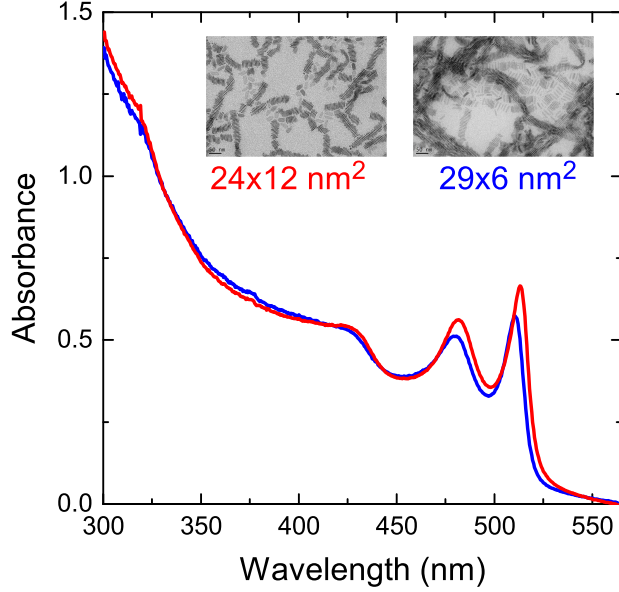

Figure 2: TEM of 29x6 nm^2 NPLs.

Figure 3: Absorption spectra of both NPLs (dispersed in PS) under consideration.

$$f_V = \frac{\ln(10)\, A(\lambda)}{L\, \mu_i(\lambda)},\qquad(1)$$

where A, L and μ_i represent the absorbance, sample's thickness and the intrinsic absorption coefficient of a specific NPL, respectively. Volume fractions in the order of $7{\cdot}10^{-5}$ (see main text) are estimated for both platelets, referring to reported μ_i from Achtstein et. al.[3] The thicknesses of both colloidal samples (entirety of NPL dispersion in solid polystyrene matrix) are 0.95 mm (24x12 nm^2) and 0.90 mm (29x6 nm^2).

Excitation Beam Diameter Determination

Figure 4 displays the excitation power dependent emission of the NPLs and CdS bulk. The observed linear dependence in the logarithmic presentation corresponds to a near quadratic power dependence. Beam A and B were switched on independently to acquire the two data sets. Since the beam profiles of beam A and B differ slightly, the same input power delivers different signals, due to the changing excitation density. However, differences in the signal can ultimately be related to the distinct beam diameters (of Beam

3

A and B) at a given position of the sample on the optical axis. This means, once the beam profiles (as functions of the optical axis z) are known, the effective beam diameter exciting a sample can be determined. To retrieve the beam diameters according to eq. 2, the mismatch parameter K (see figure 4) is evaluated. In logarithmic depiction a relative shift (here: of the data points of Beam B) of $\log(K)$ along the ordinate is done to overlay the data of Beam A and B. In the linear regime this is equivalent to a scaling factor applied to the signal generated by Beam B. Since both signals exhibit inherent dependence on the square of input intensity (see main text), the ratio of both signals can be reduced to the ratio of beam diameters and thus be linked to K.
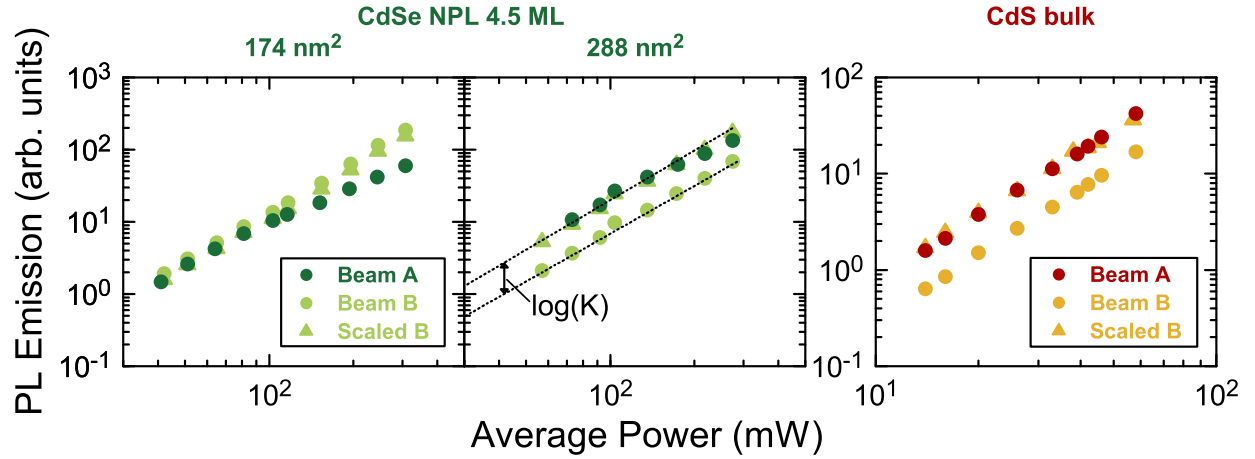

Figure 4: Collected fluorescence signal over average input power for CdSe NPLs of 174 nm^2 and 288 nm^2 area, respectively, as well as CdS bulk.

$$K = \frac{S(P_A)}{S(P_B)} = \left(\frac{w_B(z)^2}{w_A(z)^2} \right)^2 \tag{2}$$

Assuming gaussian beams, of which the functions of the beam radii $w(z)$ are known, the equation can be solved to give the position z. In turn, knowledge about the (effective) beam diameters (for A and B) can be used to plot the signal over excitation intensity (see main text, Fig. 3).
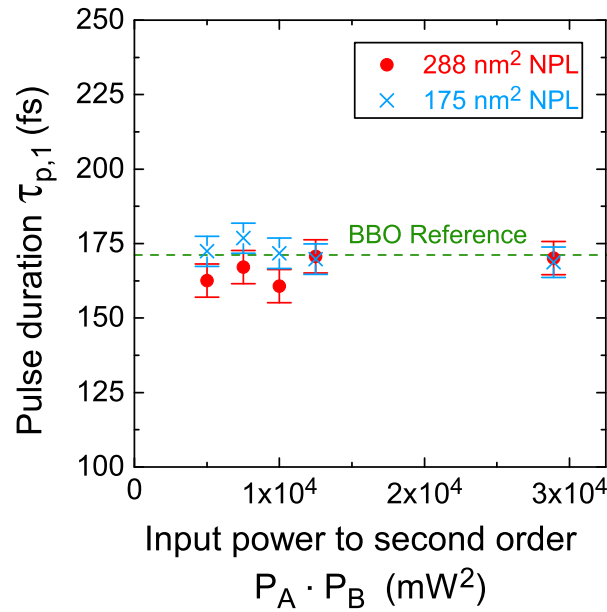
Measured pulse width vs. input power

Figure 5: Measured pulse duration vs. second order input power for two nanoplatelets (NPL) differing in size. The obtained pulse durations agree with the reference value of 171 fs given by a BBO-SHG autocorrelation measurement (depicted in green).

In order to asses the reliability of the two different NPL-autocorrelators (174 nm^2 and 288 nm^2) at diffrent input powers, we plot the results of autocorrelation measurements against the input power to second order. Since the TPA autocorrelation signal, our figure of merit, relies on the product of input powers (P_i) delivered by both beams (A and B), the pulse duration is depicted against the product of P_A and P_B. The results agree reasonably within their standard deviation among each other as well as with the BBO reference (Fig. 5). Hence the TPA autocorrelation is shown to be independent on the input power.

Fluorescence Quantum Yield of CdS Bulk

The absolute fluorescence quantum yield of CdS bulk (wurtzite) is gained by a comparative measurement with respect to Coumarin 307 (C307) in chloroform. Starting from the most general definition of fluorescence quantum yield, we are looking at the number of
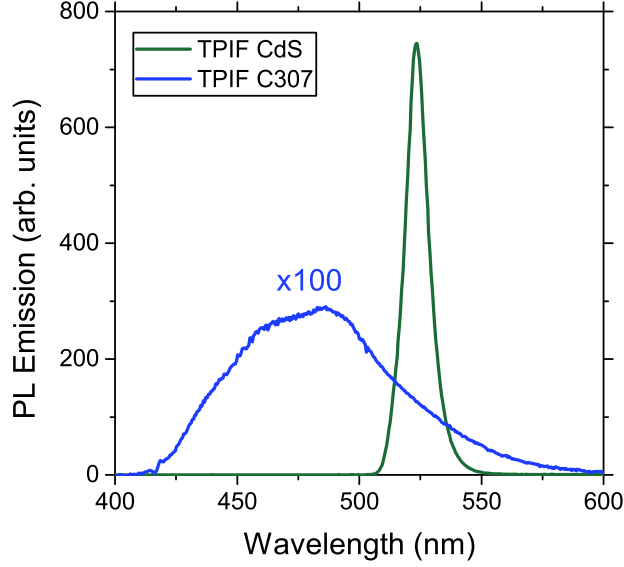
Figure 6: PL signal of CdS bulk sample and Coumarin 307 over wavelength.

fluorescence photons N_{Em} with respect to the number of initially absorbed photons N_{Abs} related via the quantum yield.

$$\eta = \frac{N_{Fls}}{N_{Abs}} \tag{3}$$

This equation can be formulated for two different materials, allowing for determination of η (sample) by comparison between a sample (s) and a reference (r).

$$\eta_s = \eta_r \frac{N_{Fls,s} \, N_{Abs,r}}{N_{Fls,r} \, N_{Abs,s}} \tag{4}$$

At first we relate the number of fluorescence photons to the integral over the luminescence spectrum F. The detected luminescence is reduced by reflection of the excitation beam (800nm) upon entering and reflection of the leaving fluorescence (see main text).

$$N_{Fls} \propto \frac{1}{(1 - R_{in})^2 \, (1 - R_{out})} \int_0^\infty F(\lambda) \mathrm{d}\lambda \tag{5}$$

To find the number of absorbed photons we start with the two photon absorption rate Γ_{Abs}. Considering only the ratio of absorbed photons as in eq. 4, it is equally valid to look at the

ratio of absorption rates.

$$\Gamma_{Abs} = \frac{\beta \, I_{exc}^2}{h \, \nu} V \tag{6}$$

where β is the TPA coefficient, I_{exc} the excitation intensity, V the corresponding volume of interest and $h \, \nu$ represents the energy per photon of frequency ν. The excitation intensity is linked to the average input power $\bar{P}$ and the area of the excitation spot, and thus to the spot radius w. As before, the experimental initial excitation intensity is to be corrected by reflection upon meeting the sample's surface.

$$I_{exc} \propto (1 - R_{in}) \, \frac{\bar{P}}{w^2} \tag{7}$$

Combining eqns. 4 to 6, assuming that V for any measurement is larger than the sampling volume of the 0.2 NA microscope objective, yields

$$\eta_s = \eta_r \, \frac{\beta_r}{\beta_s} \, \frac{\int_0^\infty F_s(\lambda) \mathrm{d}\lambda}{\int_0^\infty F_r(\lambda) \mathrm{d}\lambda} \left(\frac{\bar{P}_r \, w_s^2}{\bar{P}_s \, w_r^2} \right)^2 \frac{(1 - R_{in,r})^4 \, (1 - R_{out,r})}{(1 - R_{in,s})^4 \, (1 - R_{out,s})} \tag{8}$$

with the average Power $\bar{P}$ and effective excitation spot radius w for both sample s and reference r. Performing the calculation a fluorescence quantum yield for the CdS bulk of 0.062 ± 0.026 ($\sim$40 % deviation) is obtained. Here we referred to Xu and Webb (Ref. 4) reporting an action cross section $\eta \cdot \sigma^{(2)}$ of 19 ± 5.5 GM. For the quantum yield of C307 in chloroform we use a value of $\eta = 0.724$.[5] To calculate an effective two photon absorption coefficient β in solution, we applied the following formula

$$\beta = \frac{\sigma^{(2)} \, C_{part}}{h \, \nu}, \tag{9}$$

where the particle concentration C_{part} (m^{-3}) in the sample cuvette is determined by a

linear absorption experiment at 400 nm excitation.

$$C_{part} = C_{mol} \cdot N_A = \frac{A}{\varepsilon L} \cdot N_A \tag{10}$$

Here C_{mol}, N_A, A, ε and L denote the molar concentration, Avogadro's number, the absorbance (0.85), the molar decadic extinction coefficient after Ref. 6 ($1.85 \cdot 10^4$ mol L^{-1} cm^{-1}) and the sample's thickness (1 mm).

References

(1) Bertrand, G. H. V.; Polovitsyn, A.; Christodoulou, S.; Khan, A. H.; Moreels, I. *Chem. Commun.* **2016**, *52*, 11975–11978.

(2) Hens, Z.; Moreels, I. *J. Mater. Chem.* **2012**, *22*, 10406–10415.

(3) Achtstein, A. W.; Antanovich, A.; Prudnikau, A.; Scott, R.; Woggon, U.; Artemyev, M. *J. Phys. Chem. C* **2015**, *119*, 20156–20161.

(4) Xu, C.; Webb, W. *J. Opt. Soc. Am. B* **1996**, *13*, 481–491.

(5) Choi, K.; Lee, C.; Lee, K. H.; Park, S. J.; Son, S. U.; Chung, Y. K.; Hong, J.-I. *Bull. Korean Chem. Soc.* **2006**, *27*, 1549–1552.

(6) Brackmann, U. Lambdachrome laser dyes. 1986.